Cobot Architecture

Michael A. Peshkin, *Member, IEEE*, J. Edward Colgate, *Member, IEEE*, Witaya Wannasuphoprasit, Carl A. Moore,
R. Brent Gillespie, *Member, IEEE*, and Prasad Akella, *Member, IEEE*

Abstract—We describe a new robot architecture: the collaborative robot, or cobot. Cobots are intended for direct physical interaction with a human operator. The cobot can create smooth, strong virtual surfaces and other haptic effects within a shared human/cobot workspace. The kinematic properties of cobots differ markedly from those of robots. Most significantly, cobots have only one mechanical degree of freedom, regardless of their taskspace dimensionality. The instantaneous direction of motion associated with this single degree of freedom is actively servo-controlled, or steered, within the higher dimensional taskspace. This paper explains the kinematics of cobots and the continuously variable transmissions (CVTs) that are essential to them. Powered cobots are introduced, made possible by a parallel interconnection of the CVTs. We discuss the relation of cobots to conventionally actuated robots and to nonholonomic robots. Several cobots in design, prototype, or industrial testbed settings illustrate the concepts discussed.

Index Terms—Cobot, ergonomics, haptics, human/machine interaction, intelligent assist device (IAD), nonholonomic, passive.

I. Motivation

A. Human/Robot Teaming

OUR WORK in cobots was motivated by ergonomic and productivity issues in automobile assembly. Many aspects of automobile manufacturing have been automated, but there has been little movement toward automation of the assembly process, where subsystems such as doors, seats, and instrument panels are integrated with a painted body shell. Human workers bring capabilities that are difficult to match with automation, such as parts-picking from unstructured environments, identifying defective parts, fitting parts together despite minor shape and process variations, pushing aside interfering cable bundles or fabric, and many more.

However, recent changes in manufacturing (e.g., just-in-time, outsourcing) have led to larger subassemblies and also to a greater reliance on information systems. These major trends, together with an increasing awareness of ergonomic injuries, have created a need for mechanical assistance for human workers, and in particular for computer-controlled mechanical assistance.

The robotics community has recognized the need for *physical* teaming of human and robot in a shared workspace [10], [16]. The concept differs from force-feedback telerobotics, in which force and motion are communicated between human and robot via an information link.

Kazerooni [11] has championed *extenders*, in which both human and robot apply significant force to a payload, with the robot amplifying the human effort, much as power steering amplifies the steering effort exerted by a driver. Extenders, which may be hydraulic or electric, apply the concept to multiple degrees of freedom.

Deeter *et al.* [15] have developed a "Next generation munitions handler advanced technology demonstrator" (NGMH ATD) for heavy ($\sim$1000 kg) payloads that must be positioned precisely and quickly. These payloads are so large that the force provided by the human operator is dwarfed by the weight or inertia of the payload. Unlike extenders in which both human and machine impose substantial forces on the payload, in NGMH the human force is primarily a source of information rather than power. NGMH goes beyond teleoperation, however, because the motion of the payload is *physically* communicated to the operator through a handle connected to the payload.

B. Virtual Surfaces for Shared Control

The cobot concept, in contrast to extenders and NGMH, supposes that *shared control*, rather than amplification of human power, is the key enabler. The cobot's main function is to bring a *virtual* environment, defined in software, into physical effect on the motion of a *real* payload (and thus also on the motion of the human operator). The virtual environment may contain regions in which the operator is free to move the payload at will; other regions into which the payload cannot penetrate; smooth sliding surfaces along which the payload can slide or be drawn away; virtual forces which sum with the actual forces applied by the operator to the payload, and so on.

While there is surely an unlimited variety of interesting haptic effects that can be created within a virtual environment [19], [17], we will concentrate here on virtual surfaces as a useful example. The utility of a virtual surface can be compared to that of a straight edge or ruler. Drawing a straight line on a piece of paper, unconstrained, is a task that is done slowly and not very well. With a straight edge, the job is done faster and better. The straight edge provides physical guidance to the human operator, leaving him in charge of some aspects of motion (power and motion parallel to the edge), while taking control of other aspects of motion (motion perpendicular to the edge). A virtual surface provides shared control between computer and human operator,

but without requiring that the surface be physically embodied as a solid object, such as the straight edge.

Virtual surfaces can be conceived in a taskspace of any number of dimensions. For instance, a two-dimensional (2-D) planar taskspace may contain a one-dimensional (1-D) manifold (a curve in the plane) that forms a limiting boundary for motion in the plane. A three-dimensional (3-D) Cartesian taskspace may contain a 2-D virtual surface.

Rotational as well as translational coordinates of a taskspace may be involved in virtual surfaces. Further, one may imagine generalizing the concept to include not only unilateral surfaces (possessing an unimpeded "outside" and a prohibited "inside"), but also bilateral constraint surfaces to which motion is entirely confined. Virtual surfaces may themselves contain surfaces of still lower dimension. We will use the term "surface" in a generalized sense independent of dimensionality: surfaces need not be 2-D, nor flat.

The task of moving a dashboard assembly suspended from an x–y rail system into a car body illustrates the benefits of virtual surfaces, both due to their information content (coordinating multiple degrees of freedom) and also their ergonomic benefit. The taskspace comprises horizontal translational motion, orientation about a vertical axis, and a "roll" axis (about the long axis of the dashboard) that must be employed to prevent interference with the doorframe as the dashboard is inserted. A single fluid motion along a curved virtual surface through four-space, guided by computer, can replace a struggle to contend with four axes at once.

Maneuvering this massive payload would be a significant ergonomic problem, even if all sources of friction could be removed and if the task takes place in a horizontal plane so that lifting is not required. Redirecting a payload's motion while it is moving at constant speed is energetically neutral, but nevertheless requires large forces from the operator. Furthermore, these "steering" forces tend to involve the muscles of the back and arms, rather than the large muscles of the lower body. In the field of ergonomics, the term "inertia management" refers to such issues which arise from payload mass.

High-quality virtual surfaces can reduce the human force needed to control the motion of a massive payload. A worker can take advantage of a curved virtual surface by sliding a payload along it and allowing the forces of the virtual surface to redirect the motion of the payload, rather than the worker's own muscular forces.

C. Approaches to Virtual Surfaces

In comparing different approaches to creating virtual surfaces it would be useful to have some familiar, physical example as a "gold standard." Unfortunately, physical surfaces come in infinite variety. Thus, the gold standard for simulating surfaces found in surgery might be quite different from the gold standard for simulating mechanical assemblies. Within the realm of virtual guides for vehicle assembly, we have found the straight edge mentioned previously to be a useful standard. Thus, the properties that we seek in a virtual surface are that it be *hard* (a force perpendicular to the surface should cause little penetration of the surface), *strong* (it should be able to withstand large forces), *smooth* (the velocity of the endpoint should be tangent

to the surface at all times), *frictionless* (motion tangent to the surface should be unimpeded by the surface), and *abrupt* (at any distance away from the virtual surface, motion in any direction should be unimpeded: the transition from a "free" region to a virtual surface should be instantaneous).

Physical implementation of virtual surfaces has been approached in several ways. Powered actuators have been explored by many researchers. A detailed survey of this field, often called haptic display, is beyond our scope [8]. The approach is to use powered actuators to oppose the force of the operator whenever motion would violate a virtual surface. Backdriveable robots, with either direct-drive motors or low gearing ratios, are commonly employed. Guaranteeing stability at a virtual surface places limits on the maximum hardness of the virtual surface that can be achieved [3]. Furthermore, especially for large-scale applications, the use of powerful motors raises safety concerns.

It has also been proposed to use brakes [18], particularly those in which braking torque can be varied continuously, to prevent penetration of a virtual surface. Such brakes may be used in combination with motors, or in place of any other joint actuators. In the latter case, the robot could be entirely passive and therefore incapable of generating movement even in the event of hardware or software failure. Physical passivity has obvious advantages for safety and user acceptance.

Joint brakes have difficulty displaying virtual surfaces that have the desired property of *smoothness*. In the fortuitous circumstance that the endpoint motion caused by one joint alone is tangent to a virtual surface, that joint's brake can be left unactivated (and the joint free) while the other brakes are fully locked. This displays a strong, smooth, and frictionless surface. In the general case, however, no such special alignment will occur, and all brakes must be partially activated. Keeping the endpoint near the virtual surface despite endpoint forces requires active control of the brakes in response to small penetrations of the surface. This has proven to be difficult (although one cause may be the nonideal behavior of currently available brakes). Alternatively, the brakes can be used in a "full-on or full-off" mode, changing the physically allowed direction of endpoint motion at frequent intervals and thereby approximating the virtual surface by a sawtooth combination of allowed motions of individual joints. Not surprisingly, this results in a perceptually jagged surface.

Book *et al.* [2] have built a passive 2 degree-of-freedom (DOF) manipulator with brakes on each joint, and also a third brake on a differential connected to the two joints. The differential and its brake provide an additional mechanically-enforced high-quality virtual surface, in which the motion of the two joints is constrained to be equal when the brake is locked. It might be hoped that the difficulties of approximating an arbitrarily oriented virtual surface would be reduced by a more fine-grained set of intrinsic surfaces.

On a more fundamental level, the use of any brake involves the dissipation of energy. Even if brakes could be controlled such that the displayed virtual surfaces were smooth, sliding along such a surface would require a higher force than moving the endpoint through the free-space region adjacent to the virtual surface, in which no brakes are activated. Returning again

to our gold standard example, the straight edge, we note that the benefit is obtained from the effect of the straight edge in offering guidance, controlling the position and direction of the pencil. Impeding the pencil's progress along the straight edge, as friction would do, is undesirable. In larger scale tasks, such as moving a payload into an automobile body, the experience of purely mechanical assist devices shows that friction is a significant problem. If a guiding surface is to be of use in making such a task faster and more accurate, it must be a low-friction surface. A surface that dissipates the human operator's energy of motion may be useful as a boundary to be avoided, or to prevent collisions, but the operator is not likely to use it intentionally by sliding the payload along it.

Another approach is that of Delnondedieu and Troccaz [4], who have built PADyC, a "passive arm with dynamic constraints." Each passive joint is equipped with two unilateral clutches, by which the joint's angular velocity is mechanically constrained to lie between two limits: $\omega_1 < \omega_{\text{joint}} < \omega_2$. The reference angular velocities ω_1 and ω_2 are produced by servomotors. As the manipulator approaches a defined virtual surface, the maximum allowed joint velocities in directions approaching the surface are reduced, reaching zero as the surface is contacted. In practice, smoothness and low friction deteriorate as a surface is approached.

D. Organization of Paper

Section II explains how cobots implement virtual surfaces using transmissions, illustrated by a simple one-wheeled cobot. Section III extends the concept to higher taskspace dimensionality. The extension is achieved with multiple transmissions, which may be either rolling wheels or continuously variable transmissions (CVTs). Section IV distinguishes two interconnection topologies for multiple transmissions, one of which facilitates the injection of small amounts of power into cobots (which are otherwise passive). The power-injection architecture is illustrated with several prototype cobots. We conclude in Section V with a discussion of the relationship of cobots to conventionally actuated robots, and to nonholonomic robots, and with a review of some open questions.

II. HOW COBOTS IMPLEMENT VIRTUAL SURFACES

A. Use of Transmissions

Cobots implement virtual surfaces by using transmissions. This avoids the need for brakes or other dissipative elements, which necessarily absorb energy of motion and thus cannot provide a frictionless surface. Transmissions are energetically neutral. A rolling wheel may be considered to be a transmission, in a sense we will elaborate later.

The simplest cobot is little more than a single wheel in contact with a flat rolling surface, as shown in Fig. 1. It has a 2-D Cartesian (x–y) taskspace, parallel to the rolling surface. We will describe the essential behaviors of a cobot using this model, and then generalize to higher dimensional taskspaces and to articulated cobots with revolute joints.

The interface to the human operator is a handle mounted on top of a force sensor that is able to measure the x–y forces applied by the operator. If there were a payload, it would be just
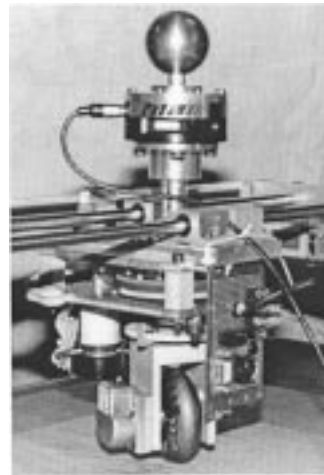

Fig. 1. A single wheel in contact with a planar rolling surface is the simplest cobot, having a 2-D taskspace. From top to bottom are the user's handle, a force sensor to measure the user's applied (xy) force, a rail system which holds the assembly upright and incorporates xy position sensors, a steering motor which can reorient the rolling direction of the wheel, and the "steerable transmission" which is central to all cobots—in this case a single free-rolling Rollerblade™ wheel. An encoder monitors the rolling speed of the wheel.

below the force sensor so that operator-generated forces could be distinguished from inertial forces of the payload.

The wheel is free to turn on its axle. There is no motor to drive its rolling motion. The wheel is held vertical by a shaft whose axis is coincident with the point of contact between wheel and rolling surface, i.e., there is no "caster" of the wheel. The wheel has a steering angle ϕ_s defined as the angle of its rolling direction from the x axis. This angle is measured by a rotary encoder (not visible). Control of the steering angular velocity ω_s is accomplished by a conventional velocity controller, which takes ω_s as input. Due to the absence of caster, action of the steering motor cannot cause taskspace motion, and forces applied to the handle do not create a torque on the steering motor. Thus, there is a decoupling of taskspace motion from steering action.

Also shown in Fig. 1 is a rail system which serves to keep the cobot upright and restrict it to its 2-D Cartesian taskspace. The rail system is instrumented with translational encoders to measure the position of the cobot within its workspace. Another rotary encoder monitors the rolling speed of the wheel, u.

This cobot, nicknamed the Unicycle, is mechanically well equipped to implement virtual surfaces. In its 2-D taskspace, a virtual surface is a curve in the plane $\mathbb{R}(s)$, where s is the path length along the curve and $\mathbb{R}(s)$ is a 2-vector in the plane (Fig. 2). Let us suppose we wish this to be a bilateral surface to which the cobot is to be confined, which we will call *path mode*. In the next section, we will address its unrestricted motion when it is not in contact with a virtual surface, *free mode*. A unilateral virtual surface is accomplished by a simple software switch between free mode and path mode, based on whether the user's applied force is directed toward the free side or the prohibited side of the virtual surface.

In the absence of errors, confining the cobot's motion to a curve in the plane requires that we measure the cobot's position s along the curve, and maintain its steering angle ϕ_s such that its rolling direction is tangent to the curve at that location. Thus,
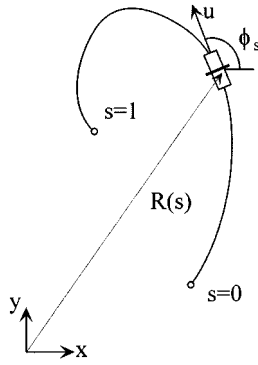
Fig. 2.   A cobot wheel following a curved virtual surface $\mathbb{R}(s)$ parameterized by a path length s. The rolling speed of the cobot wheel is u, and its steering angle (with respect to the x axis) is ϕ_s.
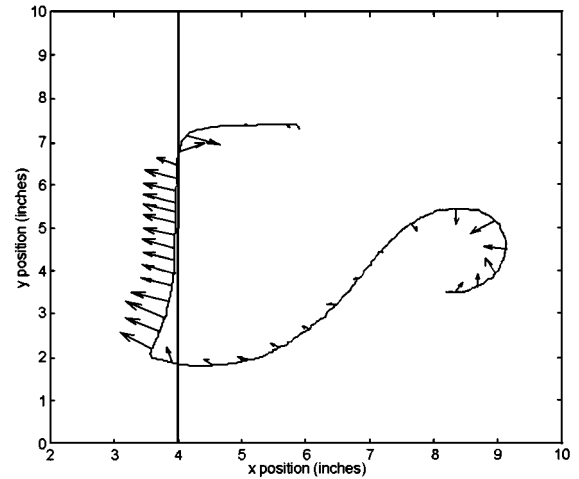

Fig. 3.   The trajectory (solid curve) and the applied user force (vectors) measured in an experiment with our prototype Unicycle cobot. A virtual surface is placed at $x = 4$ inches, with its free side on the right. Motion begins at $x = 8$ inches. Near $x = 8$ significant $F_\perp$ forces in the "inward" direction can be seen as the operator brings the cobot in a half-circle. Forces are relatively low as the cobot is moved at constant velocity toward the virtual surface. The operator force $F_\perp$ directed into the virtual surface is resisted by it, until at $y = 7$ the operator pulls the cobot away from the virtual surface, and the cobot responds by resuming free mode control [23].

open-loop control for a cobot path following a virtual surface may be accomplished by

$$\omega_s = u/\rho \qquad (1)$$

where u is the measured rolling speed of the wheel, ρ is the instantaneous radius of curvature of the virtual surface, and $\omega_s = d\phi_s/dt$ is the commanded steering angular velocity. Open-loop control is subject to an accumulation of errors, resulting in the cobot straying from the defined virtual surface. The closed-loop problem, including the transition from free mode to contact with a virtual surface, is treated in a companion paper [7].

The resulting virtual surface relies for its strength and hardness not on actuators, but on the properties of a rolling wheel. The wheel rolls freely in what we will call its *allowed direction*, while supporting large perpendicular ("skidding") loads, thus providing a low-friction virtual surface. In practice, we use Rollerblade™ wheels, taking advantage of a technology optimized for a sport that requires similar wheel properties. Virtual surface strength well over 100 pounds is attainable. Perceptually, the virtual surface may be compared to a well-greased rail, confining motion to any programmed curve in the plane.

Again, it must be appreciated that our gold standard is the straight edge. By its very mechanics, the rolling wheel does a good job of emulating a straight edge. Were it our desire to emulate compliant surfaces or surfaces with pronounced texture or friction, the Unicycle cobot would fare poorly when compared to conventional haptic devices.

B. Free Mode and Unilateral Surfaces

The two degrees of freedom of the rail system are reduced by the rolling constraint of the wheel. Kinematically, the cobot has one degree of freedom where a conventional robot x–y architecture would have two. Thus, the cobot's intrinsic mechanical behavior is close to that of an ideal virtual surface, where a conventional architecture has an intrinsic behavior close to that of free mode. One might say that, with a conventional robot architecture, a virtual surface must be actively simulated, whereas with a cobot it is the free mode that must be actively simulated, as we describe next.

Free mode is implemented by a servo loop in which the operator's applied force is measured by a force sensor, and the cobot's single degree of freedom is steered to allow motion in

the direction that the operator's force directs. Since any sort of software filter may be applied to the operator's force, we are afforded the opportunity for a great variety of haptic effects.

Ideally, free mode would be perceptually zero-friction and massless. However, the response of the cobot to the operator's force in the allowed (rolling) direction is governed not by our servo loop but by the natural behavior of the mechanical system, since it is entirely free-rolling in that direction. It has a physical mass that will dictate its acceleration in response to an applied force. Instead of masslessness, our simulated free mode will attempt to make the cobot *isotropic*: it should respond to operator forces that are perpendicular to the instantaneous allowed direction just as it does to forces parallel to that direction.

Let a coordinate system be aligned with the instantaneous allowed direction, such that the direction designated $\|$ is parallel to rolling and $\perp$ is in the perpendicular direction. Since $a_\| = F_\|/m$ is beyond our control, we desire $a_\perp = F_\perp/m$ in order to match it, i.e., to make the operator perceive the handle to have an isotropic mass. This is to be accomplished through control of the steering angular velocity ω_s. Kinematics dictates $a_\perp = u\omega_s$ where u is the measured speed in the allowed direction. The necessary control law is thus

$$\omega_s = \frac{F_\perp}{mu} \qquad (2)$$

where $F_\perp$ is the measured operator force in the $\perp$ direction. Fig. 3 shows the trajectory (solid curve) and the applied user force (vectors) measured in an experiment with our prototype Unicycle cobot.

There is a slight "hook" in the response of the cobot at rolling speed $u = 0$, because the wheel cannot be instantly steered to allow rolling in any arbitrary direction unexpectedly chosen by the operator [note the $u = 0$ singularity of (2)]. When a cobot is brought to standstill and then pushed in some new direction,

there is generally a noticeable hesitation as the wheels reorient. If, however, (2) leads to a commanded w_s within the capabilities of the steering servo, highly isotropic behavior can be achieved. In the case of the Unicycle, we have found that, at speeds of a few cm/s or faster, the behavior is qualitatively isotropic.

C. Inertia and Anisotropy Masking

Two interesting free-mode behaviors that can be accomplished in software are *anisotropy masking* and *inertia masking*. These are of practical importance in unpowered overhead rail systems, which are one form of a class of "assist devices" extensively used in materials handling. Such rail systems consist of two parallel fixed rails ("long rails") on opposite sides of a workspace. Spanning the workspace perpendicular to the long rails are one or more "bridge rails" whose ends are connected to the long rails by wheeled trolleys, so that the bridge assembly can translate along the long rails. A payload is arranged to translate along the bridge rails. Both the friction and inertia of motion along the bridge rails is less than that of motion along the long rails, because translation of the heavy bridge assembly itself is involved in the latter. This anisotropy has the result that when an operator pushes a payload in a particular direction it does not move in that direction, but instead veers closer to parallel with the bridge rail, which makes it difficult and slow to maneuver. A similar problem occurs with assist devices that use articulated arms: the kinematics of the arm affects the relationship between operator force and payload motion in a complicated way, but the operator would prefer a more intuitive, predictable, and isotropic behavior of the payload in response to his applied forces.

A large-scale cobot in the form of an overhead rail system will be described in Section IV-C. In the cobot, the allowed direction of motion is completely determined by the angle to which the wheel has been steered and is not affected by friction or inertia of the structural parts of the device. Equation (2) may be considered to be nulling the $F_\perp$ component of the operator's applied force by rotating the $\|$-$\perp$ coordinate system until the allowed direction of motion is aligned with the operator's applied force. Thus, the underlying anisotropy of the rail system's structure has no effect on the direction of motion of the payload, which is computed based on the operator's applied force.

Inertia masking makes use of the fact that the apparent mass of the payload is a result of servo-control, using (2), which is implemented in software. In other words, the term m used in (2) need not be the actual mass of the payload, but can be any *effective mass* m_{eff} that we wish it to be. If we use an effective mass much less than the actual mass, the operator's experience is that the payload is much easier to divert from a straight-line path than its actual mass would lead one to expect; its "steering inertia" has been reduced. There is no similar masking of inertia in the direction of motion ($\|$), because that inertia is a consequence of natural laws and not of computed control. The result is a strange but not unpleasant sensation that the payload is heavy to get moving (and to stop), but easy to turn. Since the large muscles of the lower body are used for propulsion, and the more easily injured muscles of the back and arms are used for turning, there may be ergonomic benefit to inertia masking.
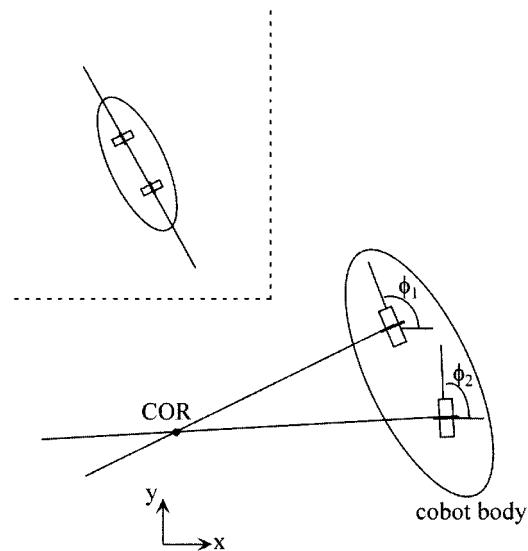

Fig. 4. The two-wheel cobot encounters a singularity whenever the wheels are coaxial, as shown in the inset. In this situation the cobot regains two mechanical degrees of freedom, since the COR may locate itself anywhere along the common axis. There is an interesting duality with conventional robots in which mechanical degrees of freedom are reduced at a singular configuration. In cobots, mechanical degrees of freedom increase at a singularity.

III. HIGHER TASKSPACE DIMENSIONALITY

A. Taskspace Dimensionality Versus Degrees of Freedom

The Unicycle cobot has a 2-D taskspace, but possesses only a single degree of freedom, due to the reduction of degrees of freedom created by the rolling constraint. The distinction between taskspace dimensionality and degrees of freedom arises from the nonholonomic nature of a rolling constraint: degrees of freedom pertains to the dimensionality of the space of available *velocities* at any instant, while taskspace dimensionality pertains to the space of *positional* configurations that the payload can reach. The cobot is not a nonholonomic robot (in the usual sense of the term), however. On a functional basis, given a present taskspace position A and a future position B, the cobot can follow any desired continuous path $\mathbb{R}(s)$ from $A = \mathbb{R}(0)$ to $B = \mathbb{R}(1)$. For a nonholonomic robot, the path $\mathbb{R}(s)$ cannot be arbitrary, but must be constructed to achieve the destination point B. Further discussion of nonholonomy will be taken up later.

We may extend the Unicycle cobot's taskspace dimensionality to three by adding a second wheel, as shown in Fig. 4, which makes control of rotational motion possible. With two rolling constraints deducted from the taskspace dimensionality of three, only one mechanical degree of freedom remains. This may be seen from the geometric construction showing that instantaneous motion of the cobot body must be describable as an angular velocity about a center of rotation (COR) in the plane, whose position is defined by the steering angles of the two wheels, ϕ_1 and ϕ_2.

Since the cobot has only a single mechanical degree of freedom, the operator has direct control only of speed, and the computer governs direction by steering. The computer can therefore moderate the operator's authority over direction through software interpretation of the operator's applied forces, as measured by a force sensor. This division of control would
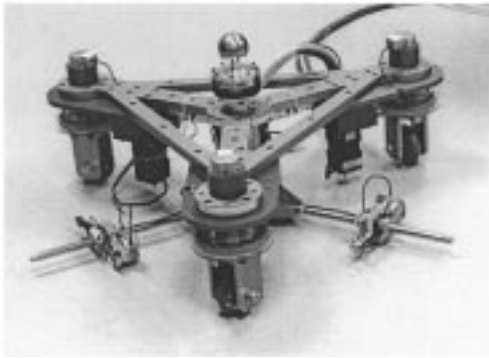
Fig. 5.   In the *Scooter* prototype shown, three small planimeter wheels are used to infer the rolling speed of the steered wheels. Rolling speed could have been measured directly on each rolling wheel, as was done with the Unicycle cobot. However, placing an encoder on a steered wheel creates a problem in which the wire from the encoder winds up around the steering shaft as the wheel is steered, thus limiting the range of steering angles to a few revolutions. In practice, we have found an unrestricted steering angle to be important. Other solutions besides planimeter wheels are also possible. The operator's handle and force sensor are located on the stalk at the center of the cobot, although they can be located anywhere with appropriate conversion of the force/torque vector.

be lost if the cobot had two mechanical degrees of freedom: the operator would have some physical control over direction as well as speed.

To avoid the singular configuration shown in Fig. 4, we have built the 3-D planar taskspace cobot as a three-wheeled device as shown in Fig. 5. When two of the wheels are coaxial, the third wheel resolves the COR degeneracy. It has the additional practical advantage that the cobot can stand on its own without a rail system. In operation, the steering of the three wheels is coordinated so that all three axes intersect at a point. Without this agreement the cobot would be immobile.

The three-wheeled cobot, nicknamed "Scooter," is able to implement convincing unilateral virtual surfaces as well as free mode in its x–y–θ taskspace. Payloads of several hundred pounds are unproblematic. Human operators interacting with Scooter find speeds up to about 2 m/s to be comfortable, and the limit appears to be one of human agility. General Motors has built a three-wheeled cobot patterned after Scooter, which is shown in Fig. 6.

While Scooter is conceptually very similar to the one-wheeled Unicycle cobot, several nontrivial kinematic and control results are needed to generalize (1) and (2) for free-mode and path-mode control, respectively. These are part of a general theory described in the companion paper [7].

In addition to unilateral virtual surfaces and free mode, we have demonstrated bilateral virtual surfaces or "path mode." In path mode, the operator's applied force is ignored by the software, and the force sensor is not needed.

B. Revolute Joints

The cobots above have planar taskspaces (x–y or x–y–θ) because the rolling surface they use is planar. Since an articulated design with revolute joints has proven to be a versatile robot architecture, we now describe extension of the cobot to revolute joints.

The rolling wheel in the cobots above may be thought of as a *translational transmission element*. A transmission holds

Fig. 6.   GM's cobot is a rugged yet highly maneuverable device. It assists in removing doors from newly painted auto bodies prior to assembly of the cabin. This task was chosen because it was both difficult and slow for workers to remove the doors manually without marring the surfaces: the curvature and styling of the body panels is such that a specific "escape trajectory" is needed to remove the door safely. Human versatility and dexterity are still very important in other phases of the task; this is not a task that should be fully automated. The door-unloader cobot glides easily on servo-steered Rollerblade wheels with only a few pounds of operator force. During some task phases the operator controls position while the cobot controls orientation, aligning itself to the car body or to the door rack across the walkway as appropriate. In close-approach phase a virtual surface is created close to the vehicle's rocker panel, guiding the cobot to the correct location to grip the door without colliding with the vehicle. The "escape trajectory" is executed in path mode. When crossing the walkway the cobot is in free mode, giving the operator direct and intuitive control over both translation and orientation.

one translational or angular speed in proportion to another. The rolling wheel may be thought of as a device that relates the x translational velocity of a certain point of a body to its y translational velocity, and holds those velocities in proportion. The proportion is adjustable by steering the wheel: we have $v_y/v_x = \tan\phi_s$, where ϕ_s is the steering angle of the wheel. Thus, a steerable passive rolling wheel formally falls in the class of kinematic mechanisms known as *continuously variable transmissions*, or CVTs. Cobots with revolute joints require a mechanical element analogous to the rolling wheel, but which relates a pair of angular velocities (rather than translational velocities). Such a device is also a CVT.

There are a great number of CVT designs that hold two angular velocities in proportion, with $\omega_2/\omega_1 = c$. Reference [1] gives a readable survey and introduction, and the patent literature is a rich source.[1] We will express the transmission ratio c as the tangent of an angle ϕ_s to maintain an analogy to the rolling wheel. Just as for the rolling wheel, for use in a cobot we require the ability to rotate the transmission angle ϕ_s without limit, through multiple revolutions. In other words, the transmission ratio c must be smoothly adjustable through all possible values, including positive values, negative values, 0, and ∞. CVTs having a range of transmission ratios that includes zero are usually called infinitely variable transmissions, or IVTs. The CVTs of interest to us are thus a subclass of IVTs. Of the many CVT designs that have been described in the literature, only a handful have a full range of transmission ratios [12], [5], [9]. These are variations on the same basic concept. We develop it

---

[1]Of particular interest are U.S. patents 1850189, 2100629, 2727396, 2931234, 3071018, and 3 248 960.
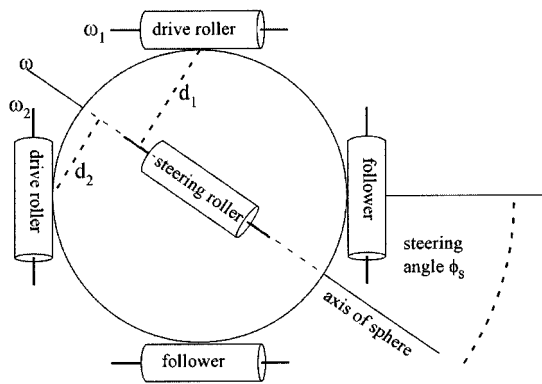
Fig. 7. Conceptual model of a continuously variable transmission (CVT) suitable for use in coupling pairs of revolute joints, holding their angular velocities in a ratio $\omega_2/\omega_1 = \tan(\phi_s)$, where transmission ratio $\tan(\phi_s)$ is "steerable" under computer control. In the drawing, the angular velocities of the drive rollers are ω_1 and ω_2, and the ratio of them is controlled by the angle of the steering roller which sets the axis of rotation of the sphere. The follower rollers serve only to confine the sphere.
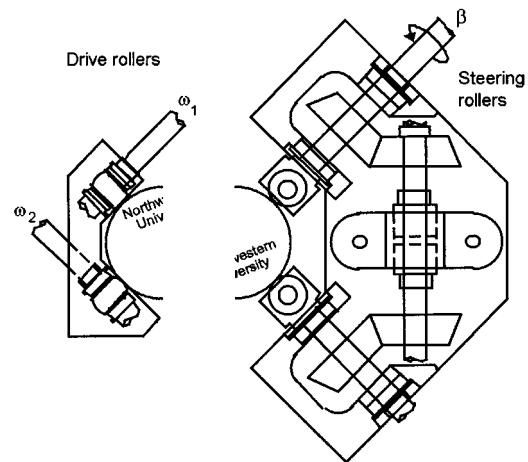

Fig. 8. A CVT of a form that is analogous to the steered rolling wheel. The angular velocity ratio of the two drive rollers is controlled by the angle set on the steering rollers. The left half of the drawing should be turned 90 degrees about a horizontal axis so that the four rollers touch the central sphere at the corners of a tetrahedron. The bevel gear mechanism on the far right serves to synchronize the angles of the two steering rollers. The axes of the two steering rollers are rotated in opposite directions by this mechanism. (The angle $\beta = 0$ shown here is related to ϕ_{12} in the text by $\beta = \phi_{12} - \pi/2$.)

first in an easily explained but mechanically suboptimal form, and then in a mechanically preferable form.

The simpler form is shown in Fig. 7. It consists of a sphere caged by six rollers, with the rollers arranged as if on the faces of a cube surrounding the sphere. Each of the six rollers is pressed in toward the center of the sphere by an externally applied force F_{preload}. The force F_{preload} serves to keep each of the rollers in rolling contact with the sphere. We do not show the frame that holds the rollers, nor the bearings that allow the rollers to turn, nor the springs which supply the force F_{preload}.

Two of the rollers are considered *drive rollers*. These are the ones that interface to other parts of a machine that incorporates the CVT. These drive rollers have angular velocities ω_1 and ω_2. Two other rollers, diametrically opposite the drive rollers, are *followers*. They serve only to confine the sphere and to apply the force F_{preload}. They rotate with angular velocity ω_1 and ω_2 also, but this rotation is not used. These four rollers (two drive rollers and two followers) have axes of rotation that all lie in a single plane, and this plane passes through the center of the sphere.

The remaining two rollers are *steering rollers*, at the top and bottom of the sphere. The steering rollers can turn freely on their axes. (Only the top steering roller can be seen in Fig. 7, as the bottom steering roller is hidden beneath the sphere. The bottom steering roller is oriented identically.) Unlike the drive rollers and followers, the axis of rotation of the steering rollers is adjustable. The angle that the axis of the steering roller forms, with respect to the horizontal, is the steering angle ϕ_s. The mechanism which allows us to vary the steering angle, and which keeps the steering angles of the top and bottom steering rollers in agreement, is not shown.

The kinematics of the rotational CVT may now be understood as follows. Consider all possible axes of rotation of the sphere. The sphere must be in rolling contact with all six rollers. Since the center of the sphere is stationary, the sphere's axis of rotation must pass through its center. Rolling contact between the sphere and a given roller requires that the axis of the sphere lies in the plane containing the axis of the roller, and also passing through the center of the sphere. Each roller-sphere pair forms such a

plane. (The planes for the followers and the bottom steering roller can be ignored, by symmetry.)

The axis of rotation of the sphere must be the intersection of the three planes demanded by the two drive rollers and one steering roller. Such an axis exists: it is in the plane of the paper, passing through the center of the sphere, and parallel to the axis of the steering roller. It is labeled "axis of sphere" in Fig. 7.

Now consider the linear velocities of the points of the sphere that contact a drive roller. If the radius of the rollers is R_{roller}, the velocities of these points of contact are $\omega_1 R_{\mathrm{roller}}$ and $-\omega_2 R_{\mathrm{roller}}$, perpendicular to the paper. If the angular velocity of the sphere (about its axis identified above) is ω, and the distances from that axis to the points of contact are d_1 and d_2, then the velocity of the points of contact can also be computed as $d_1\omega$ and $-d_2\omega$. Equating $\omega_1 R_{\mathrm{roller}} = d_1\omega$ and $-\omega_2 R_{\mathrm{roller}} = -d_2\omega$ we find $\omega_2/\omega_1 = d_2/d_1$. Note from the geometry that $d_2/d_1 = \tan(\phi_s)$. Thus we have established an adjustable transmission ratio between the angular velocities of the two drive rollers

$$\frac{\omega_2}{\omega_1} = \tan\phi_s \qquad (3)$$

where ϕ_s can be interpreted as the steering angle, just as for a rolling wheel.

Figs. 8–10 show a modified rotational CVT, which has many practical advantages. Its principle of operation is the same as that of Fig. 7, but it requires only four rollers instead of six. (Four is the minimum number of point contacts needed to confine a sphere.) The two follower rollers are thus eliminated. The rollers contact the sphere at four points describing the corners of a tetrahedron. It is not a regular tetrahedron, but rather a stretched one, such that the angle subtended by the points of contact of either pair of rollers with the center of the sphere is 90 degrees. This facilitates manufacture. (For a regular tetrahedron, this angle would be 108 degrees).

Fig. 9. A prototype of the tetrahedral CVT. The drive rollers are attached to the two shafts on the left (which are perpendicular to each other). The steering rollers are on the right side, and a portion of the gear mechanism which synchronizes the steering rollers is also visible.
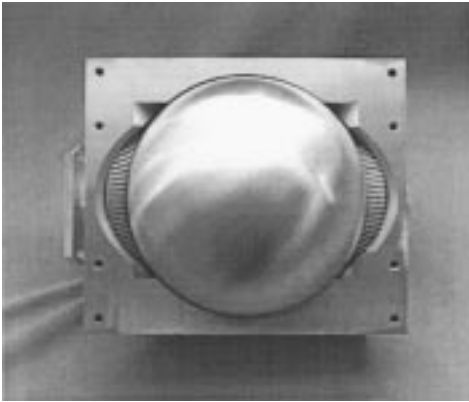

Fig. 10. A rugged and compact design for the tetrahedral CVT, shown with the top half removed. (Courtesy S. O. Colgate, University of Florida.)

The rollers no longer need to be independently preloaded. Instead, a rigid frame holds the two drive rollers, and another rigid frame holds the two steering rollers. These two frames can be simply drawn together by a spring, which will apply the same force F_{preload} to all four contacts.

Finding the axis of rotation of the sphere is more difficult for the tetrahedral arrangement shown in Fig. 8 than for the cubic arrangement of Fig. 7. The axes of the drive rollers are perpendicular and coplanar, just as they were in the cubic arrangement. The axes of the two steering rollers are not parallel, as they were in the cubic arrangement. They are in fact coplanar, but the plane that they share does not in general contain the center of the sphere. Rather, the two distinct planes formed by the axis of each steering roller with the center of the sphere intersect one another, and that line of intersection is the axis of rotation of the sphere. It lies in the plane of the drive rollers.

Careful geometry [13] yields the transmission ratio

$$\frac{\omega_1}{\omega_2} = \frac{\sin(\phi_{12}) - \sqrt{2}\cos(\phi_{12})}{\sin(\phi_{12}) + \sqrt{2}\cos(\phi_{12})} \qquad (4)$$

where ϕ_{12} is the steering angle of the steering rollers. The transmission ratio ω_1/ω_2 assumes a full range of values ($-\infty$ through $+\infty$) as the steering angle ϕ_{12} is changed.

Calculations and experimental results for the kinematics and the slip properties of CVTs may be found in [13], [6]. Additional work on spherical CVTs may be found in [12].

C. Use of the CVT in Revolute-Jointed Cobots

The conceptual design shown in Fig. 11 illustrates the use of CVTs as the central transmission elements of a 3-D taskspace (x–y–θ) cobot, having revolute joints. The three links have angular velocities ω_1, ω_2, and ω_3, each measured with respect to the previous link's angular velocity. One CVT couples ω_2 to ω_1 by a transmission ratio $\omega_2/\omega_1 = \alpha_{21}$, and a second couples ω_3 to ω_2 by a transmission ratio $\omega_3/\omega_2 = \alpha_{32}$. Thus, ω_3 is also mechanically coupled to ω_1 by a transmission ratio which is the product of the two: $\omega_3/\omega_1 = \alpha_{32}\alpha_{21}$. The transmission ratios α_{21} and α_{32} are servo-controlled, just as the steering angles of the wheels in the planar cobots above were servo-controlled.

The first two links alone, with the second CVT and link 3 removed, could be considered a 2-D taskspace revolute cobot similar to the Unicycle, while the three-link cobot as shown has a planar taskspace like that of Scooter.

In free mode, a force sensor at the endpoint measures the operator's applied force-and-torque vector $\boldsymbol{F}_{\mathrm{taskspace}}$, which is converted to a jointspace description by a conventional Jacobian transformation $\boldsymbol{F}_{\mathrm{jointspace}} = \boldsymbol{J}^T \boldsymbol{F}_{\mathrm{taskspace}}$. An inertia matrix $\boldsymbol{M}$, which need not correspond to actual mass, and a scalar speed u are required to identify the appropriate steering angular velocity of the transmission angles ϕ_{21} and ϕ_{32}, which in turn control the transmission ratios α_{21} and α_{32}.

Endpoint motion instantaneously tangent to a defined virtual surface occurs for a particular ratio of joint angular velocities $\omega_1 : \omega_2 : \omega_3$. This ratio can be enforced mechanically by appropriate settings of α_{21} and α_{32}. As the endpoint moves, the instantaneous tangent to the virtual surface changes and the required ratio $\omega_1 : \omega_2 : \omega_3$ changes.

D. Two Models of Higher Dimensional Cobots

In principle, the structure above could be extended to any number of links, even to a 6R robot. It has the disadvantage that the transmissions communicate with one another in a serial chain, as illustrated in Fig. 12. In the figure, the nodes represent distinct angular velocities of the joints, ω_1, ω_2, ω_3. The blocks represent CVTs, each of which couples two angular velocities according to a transmission ratio α that is shown as an input to the CVT. The angular velocities map to an endpoint velocity via the ordinary Jacobian of the robot.

A disadvantage of a serial chain is that the transmission ratio constraining nonadjacent angular velocities (ω_1 and ω_3 in Figs. 11 or 12) is a product of the transmission ratios of all intervening CVTs (e.g., CVT_{21} and CVT_{32}). This leads to an accumulation of errors and also to a degeneracy when any intervening angular velocity is required to be zero (in this example, when $\omega_2 = 0$). The degeneracy is much like that of the two-wheeled cobot illustrated in the inset of Fig. 4: when wheels become coaxial the number of mechanical degrees of freedom increases from one to two. Here, any value of the angular velocity triple $\omega_1 : 0 : \omega_3$ becomes mechanically permitted.

An alternate structure couples each joint's angular velocity individually to a common one, which we will denote an *internal*
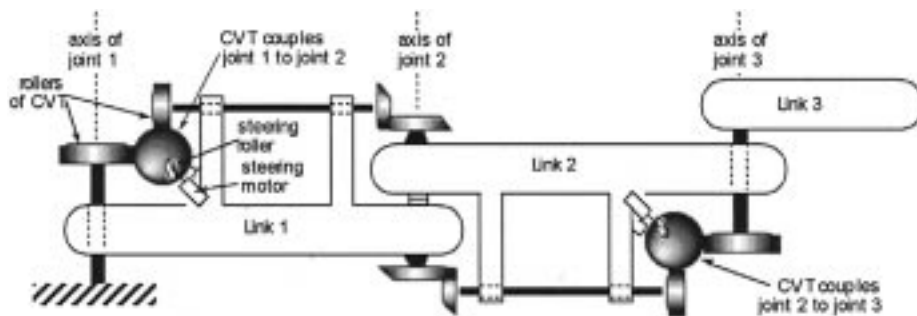
Fig. 11.   Conceptual model of a planar-taskspace (x–y–θ) cobot with revolute joints, whose angular velocity ratios (ω_2/ω_1 and ω_3/ω_2) are controlled by CVTs. Note that the lower and upper gears or rollers on the line labeled "axis of joint 2" are rigidly attached to link 1 or link 2, respectively.

motion, indicated as ω_0 in Fig. 13. If the taskspace dimensionality is n, the serial chain structure above required $n-1$ CVTs and $n-1$ control inputs. The alternate *parallel*[2] structure diagrammed in Fig. 13 requires n CVTs and n control inputs. The internal motion ω_0 may be considered to be an additional member of jointspace, which now has dimensionality $n+1$. Unlike the other jointspace components $\omega_{1,2...}$, the internal motion ω_0 is not coupled to a taskspace motion. It is purely the motion of an internal part of the cobot. In both the serial and the parallel structures the number of mechanical constraints imposed by the CVT transmission ratios lowers the number of degrees of freedom to one.

The parallel structure eliminates the degeneracy of the serial chain structure, at the expense of one additional CVT and its control input. An additional benefit is convenient access to the *internal motion*, which we consider next. Section IV-B includes a physical example of a cobot possessing an internal motion.

IV. POWERED COBOTS

A. The Internal Motion

Let v be the taskspace velocity, expressed as a configuration-space vector. (For a high workspace dimension cobot, v could include both translational and rotational axes.) Let ω be the jointspace velocity, e.g., $\omega = (\omega_1, \omega_2, \omega_3)$. v and ω are related by the usual configuration-dependent Jacobian which reflects the kinematics of the links of the robot, $v = J\omega$. Each joint's angular velocity is proportional to the scalar velocity ω_0 of the common *internal motion*: $\omega_j = \alpha_j\omega_0$, or in vector form $\omega = \alpha\omega_0$, where α is a vector of the n transmission ratios, e.g., $\alpha = (\alpha_{10}, \alpha_{20}, \alpha_{30})$. Thus, we have $v = \omega_0 J\alpha$: the taskspace velocity has a direction which is that of $J\alpha$ and a magnitude[3] which is the product of ω_0 and $|J\alpha|$.

J and α may be computed from the kinematics of the links and of the CVTs, respectively, and α is under computer control. $J\alpha$ determines the instantaneous direction of motion in taskspace that corresponds to the single mechanical degree of freedom of the cobot. That kinematically allowed direction is

$$\hat{v}_{\parallel} = \frac{J\alpha}{|J\alpha|}. \tag{5}$$

[2]It should be noted that a parallel CVT structure is in no way related to parallel kinematics. Indeed, the cobot pictured in Fig. 15 features a parallel set of CVTs connected to a serial kinematic linkage.

[3]A norm for mixed-unit taskspace vectors (translations and rotations) must be chosen, but nothing in our discussion depends on which norm is used.
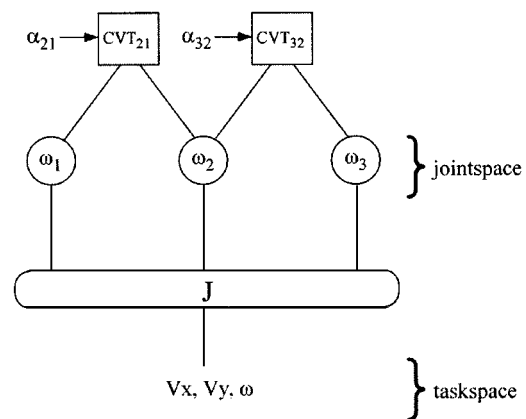

Fig. 12.   The CVTs of the revolute cobot sketched in Fig. 11 communicate with one another in a *serial* chain as diagrammed. The control inputs to the CVTs are α_{21} and α_{32}. Jointspace as well as taskspace are 3-D. Each CVT places one mechanical constraint on the three jointspace variables, reducing the number of mechanical degrees of freedom to one.
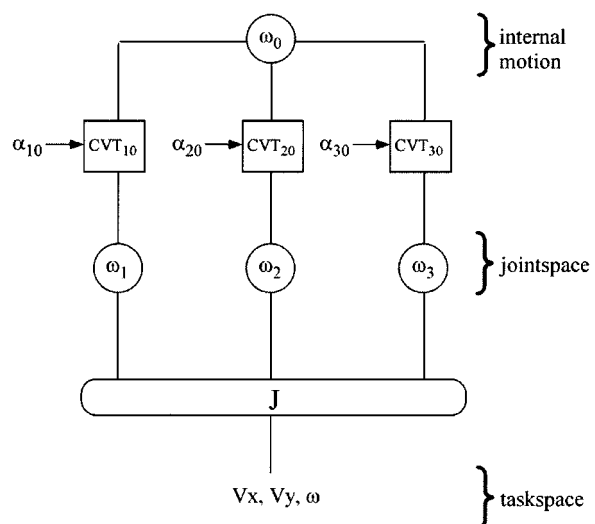

Fig. 13.   An alternate structure for cobots places the CVTs in a *parallel* configuration diagrammed here. Taskspace remains 3-D, but jointspace may be considered to be expanded to include an *internal motion* ω_0 through which the other jointspace variables communicate. One additional CVT is required. Each CVT places one mechanical constraint on the four jointspace variables, reducing the number of mechanical degrees of freedom to one.

The scalar velocity ω_0 is now conveniently accessible as the motion of a particular mechanical element of the cobot, independent of the instantaneous direction of that motion in taskspace,
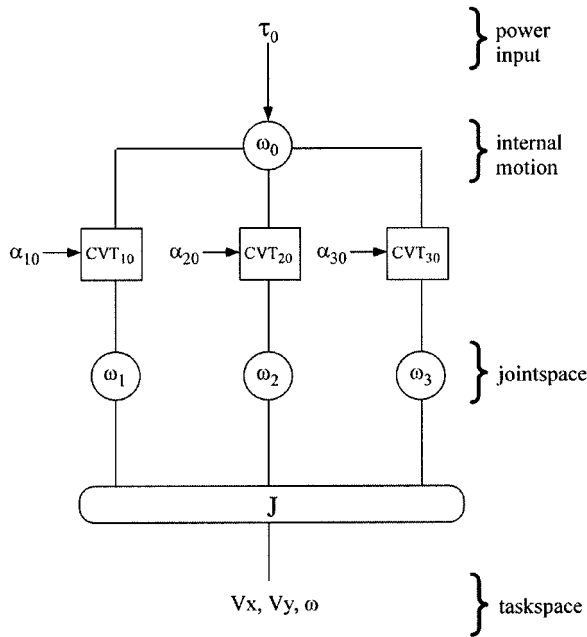
Fig. 14.   Structure of a powered cobot. The parallel CVT arrangement makes an internal motion ω_0 accessible, which is directly related to the forward speed of the endpoint of the cobot in the single direction that is mechanically allowed at a given moment. A "power-assist" torque input (or a braking torque) τ_0 may be applied to the common internal motion, to drive or impede the forward motion.

$\hat{\boldsymbol{v}}_\|$. It is directly proportional to the scalar speed and sense (positive or negative) of the endpoint of the cobot. Measurement of ω_0 is analogous to measurement of the rolling speed of the Unicycle cobot, a measurement which was made inconvenient by steering of the wheel.

Furthermore, the internal motion is mechanically coupled to the operator and payload's forward motion in the kinematically allowed direction $\hat{\boldsymbol{v}}_\|$. The ratio of these two speeds is

$$\frac{|\boldsymbol{v}|}{\omega_0} = |\boldsymbol{J}\boldsymbol{\alpha}| \qquad (6)$$

where $|\boldsymbol{J}\boldsymbol{\alpha}|$ may now be interpreted as a transmission ratio from the internal motion to taskspace motion. A *powered* cobot may apply a motor torque (or braking torque) to the internal motion, and thus help or hinder the operator in moving the payload in the mechanically allowed direction. The structure of a powered cobot is diagrammed in Fig. 14.

All of the control inputs are computed from measurements of the operator's force $\boldsymbol{F}$ applied at the endpoint. Following the notation of Section II-B, the projection of $\boldsymbol{F}$ onto the allowed direction $\hat{v}_\|$ will be denoted $F_\|$. Proportional amplification of the operator's applied force may be accomplished via servo control as simple as
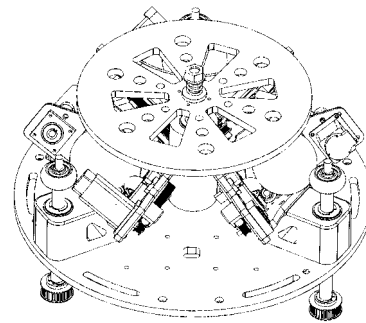
$$\tau_0 = g F_\| \qquad (7)$$

where g is a gain factor. If desired, the transmission ratio $|\boldsymbol{J}\boldsymbol{\alpha}|$ (relating internal motion to taskspace motion) can be used for impedance matching of the drive motor to the payload.
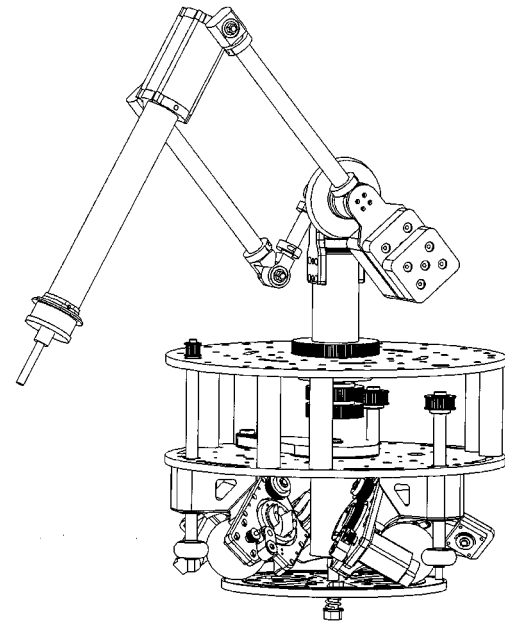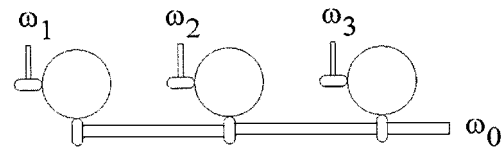
Fig. 15.   A powered cobot with a three revolute axes, presently under construction. All three CVTs are in a stationary frame [lower part of (a)] to minimize the moving mass of the pantograph-style arm. Three CVTs are used, each coupling one of the axes of motion of the arm to a common "power wheel" carrying the internal motion ω_0. (b) We show schematically how the three CVTs share a common motion, that of the shaft. (c) A view from below (a), showing the actual layout of the three CVTs in contact with the power wheel. The power wheel is also direct-driven by a servomotor.

B. A Three-Dimensional Taskspace Powered Cobot

A concrete example of a powered cobot using the parallel CVT arrangement diagrammed in Fig. 14 may be a useful illustration of the above ideas. Such a cobot, presently under construction, is illustrated in Fig. 15. It has three revolute joints and an x–y–z workspace of about 1 m radius. The pantograph-style arm allows all three CVTs to remain in a stationary frame, minimizing the moving mass of the arm. The arm linkage is described more fully in [14].

The three CVTs each couple one revolute joint to a common internal motion ω_0, which is carried by the "power wheel" at the bottom of Fig. 15. The CVTs are somewhat integrated with the
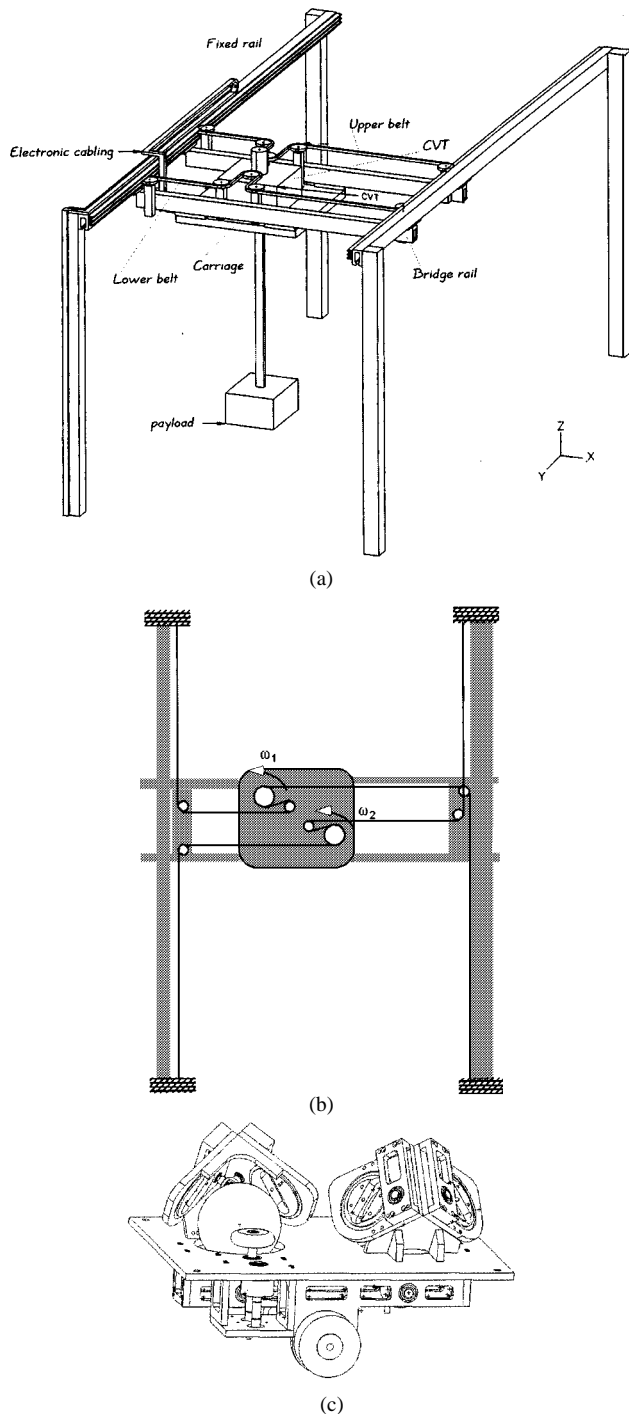
(a)

(b)

(c)

Fig. 16. A gantry-style cobot based on typical overhead rail systems used in materials handling. A single wheel could have been used to couple x and y motion of the carriage, but a rolling surface is not practical. Instead, belts [shown in (a) and (b)] couple translational motion of the carriage to rotational motions ω_1 and ω_2. The parallel CVT configuration shown in Fig. 14 is used, comprising (c) two CVTs coupled to each other by a short belt (not shown) that carries the internal motion ω_0. A servomotor also drives the short belt, and is thus able to inject power into (or brake) the forward motion of the cobot.

power wheel. Rather than having two fully-developed rotating shafts carrying motions ω_i and ω_0 (for $i = 1, 2, 3$), the power wheel contacts the central sphere of each CVT_{i0} directly, as illustrated on the right side of Fig. 15. A motor is directly coupled to rotation of the power wheel ω_0 and may be used to assist or impede the endpoint motion of the cobot.

C. A Two-Dimensional Taskspace Powered Cobot

Shown in Fig. 16 is a 2-D taskspace powered cobot based on an industrial overhead-rail system. This cobot was built at Collaborative Motion Control, Inc., under contract to Ford Motor Company, and has undergone testing at Ford's Advanced Manufacturing Test Facility.

The taskspace of this cobot is planar and 2-D, identical to that of the Unicycle cobot which used only a single steered rolling wheel as its transmission element. However, in a plant environment, a large unobstructed rolling surface is often impractical, and so we have instead used a more compact design based on revolute CVTs. Jointspace thus consists of two angular velocities ω_1 and ω_2, which are coupled to the x–y taskspace via the belt arrangement shown in Fig. 16(b). The ends of the belt [at the four corners of Fig. 16(b)] are fixed, and it may be observed that y motion of the carriage (upward in the figure) causes clockwise rotation of ω_1 and ω_2, while x motion of the carriage causes ω_1 and ω_2 to have opposite sign. ω_1 and ω_2 are coupled by a CVT assembly mounted on the carriage, thus controlling the translational freedom of the carriage itself.

For the CVT assembly we have used two CVTs in the parallel configuration discussed above, rather than the minimum requisite single CVT, in order to make the injection of power possible. The CVTs are mounted on the payload carriage as shown in Fig. 16(c), and share an internal motion ω_0 that is carried by a short belt, not shown. A small 200-W motor drives or is driven by this internal motion.

The drive motor is adequate to overcome the inherent friction of the rail system and belts, and to considerably ease the human effort required to bring a 150-kg payload from rest to a speed of 2 m/s. For safety reasons, one would not want a motor of greater than human power. By comparison, turning the payload through a 90-degree bend, with a turning radius of 30 cm, when it is travelling at 2 m/s, would require a 4000-W motor, if our virtual walls relied for their strength on motors rather than CVTs.

V. Discussion

A. Relation of Cobots to Conventionally Actuated Robots

A powered cobot of taskspace dimension n requires $n + 1$ motors, one more than would a conventional robot of the same dimensionality. Of the cobot's $n + 1$ motors, however, n are used to select the single kinematically allowed direction of motion within the n-dimensional taskspace, which they do by adjusting ("steering") the transmission ratios of CVTs. In principle, this is a signal-level action, rather than a power-level action, because workspace motion is mechanically decoupled from steering motion. In practice, some power is required to adjust a CVT, but low-power, low-speed, low-performance motors may be used.

Only one of the $n + 1$ motors is a power-level actuator. (For passive cobots, this actuator is absent.) Regardless of the direction of motion in taskspace, that one motor is used to amplify (or impede) human effort. Smooth and safe amplification of human effort has been difficult to achieve in multiple dimensions. The cobot architecture reduces the problem to a single degree of freedom, where it becomes manageable.

Difficulties of smoothness and stability aside, if a robot is to produce a virtual surface its motors must be capable of exerting the necessary forces to defend that surface. The maximum force that can be exerted by a robot can be traced to a maximum motor torque. In contrast, virtual surfaces produced by cobots are defended not by the strength of actuators, but by the mechanical strength of transmissions, which are energetically neutral devices. Therefore the motors used in a cobot may be far smaller than the strength of its virtual surfaces would seem to imply.

The essential structural difference between robots and cobots is that cobots have a single degree of freedom. The terms *degrees of freedom* and *taskspace dimensionality* have often been used interchangeably, but here we must draw the distinction sharply: *degrees of freedom* refers to the dimension of the space of velocities that is mechanically allowed by the robot's (or cobot's) mechanism at a particular instant. *Taskspace dimensionality* (n) refers to the space of endpoint poses (position and orientation) that can be reached over time.

Although cobots have only a single mechanical degree of freedom, they nevertheless have a full complement of control inputs. For taskspace dimensionality n, an unpowered cobot with a serial chain of transmissions requires $n-1$ transmissions, and a cobot with a parallel structure requires n transmissions. There is one control input for each transmission. For a powered cobot, the motor which adds power in the allowed direction of motion is an additional control input that may be added to the above count. The human operator's input of force in the allowed direction could also be considered a control input, although of course it is not under computer control.

Although *mechanically* only a single direction of motion of the endpoint is allowed at any instant, because of the full set of control inputs one also has a software-mediated ability to steer that single direction to lie anywhere within the n-dimensional taskspace. One might say that the *apparent freedom* of the cobot to move in any direction at any instant is a "simulated" freedom. In comparison, a fully-actuated robot has n mechanical degrees of freedom. If by use of its actuators the robot can confine its endpoint to a lower dimensional subspace or even to a path, despite user-forces perpendicular to that subspace, one might say that it is the *apparent constraint* which is simulated.

B. Relation of Cobots to Nonholonomic Robots

CVTs and rolling wheels are nonholonomic devices,[4] and the relationship of cobots to nonholonomic robots is worth exploring. A considerable body of work has developed around path planning for nonholonomic robots.

Nonholonomic robots are *underactuated*: they have fewer actuators than they have configuration space dimensions. For instance, a tractor-trailer requires four configuration space variables to describe its position (x, y), orientation, and the angle of the cab relative to the trailer, but it has only two actuators: speed and steering angle. Parking a tractor-trailer requires con-

siderable skill in order to create a path that achieves the desired configuration; the path planning problem from an initial pose A to goal pose B is nontrivial. Were it not for the nonholonomy of rolling, a tractor-trailer would be forever confined to a 2-D subset of its 4-D configuration space.

The language of nonholonomic robots does not distinguish between power-level and signal-level actuators. We would consider the tractor-trailer to have two control inputs, speed and steering, the former requiring a power-level actuator and the latter requiring merely signal-level control of a transmission ratio (its steering angle). Notice that the path planning problem would be no different if the front wheels were independently driven by two power-level actuators, rather than steered and driven mutually. Here we will use the term *underactuated* to mean that the number of *power-level* actuators is fewer than the configuration space dimensionality. We will use the term *undercontrolled* to mean that the number of *control inputs* (whether power-level or signal-level) is fewer than the configuration space dimensionality.

Nonholonomic robots are *undercontrolled* as well as underactuated. The space of available velocities is of lower dimension than the configuration space. The challenge is then to design a trajectory that nonetheless reaches a desired goal configuration, despite a severe restriction on available directions of motion. In contrast, cobots are underactuated but *fully controlled*: the number of control inputs is equal to or greater than the configuration space dimension. (In the case of unpowered cobots the human user's applied force, an exogenous input, should be counted amongst the control inputs.) Thus, the interesting challenges of nonholonomic path planning do not apply to cobots.

Soerdalen, Nakamura, and Chung [20] have investigated a nonholonomic robot arm that is both underactuated and undercontrolled. Its nonholonomy derives from a novel joint mechanism which bears a striking visual similarity to the CVTs described here, due to the use of a central sphere. The joint produces a constraint much as a CVT does, reducing by one the number of mechanical degrees of freedom of the robot. Unlike a CVT, one does not have software control of that constraint; the joint has no control input.

To summarize, a conventional robot is *fully actuated*, with a number of power-level actuators equal to or greater than the configuration space dimension. A nonholonomic robot is underactuated and undercontrolled. A cobot is underactuated, but fully controlled. Cobots and nonholonomic robots make use of nonholonomic devices (wheels or CVTs) for the same purpose: to access a high-dimensional configuration space despite underactuation.

C. Applications

Cobots have been well received in the automotive industry. Prototype assembly cobots have been tested at General Motors and at Ford Motor Company. Tasks investigated have included door removal on a moving assembly line, a truck bumper transfer operation, and seat loading on a moving assembly line. The door removal task is described in detail in [24]. These prototype systems have been successful in demonstrating the potential benefits of assembly cobots, including improved

---

[4]One definition is that a holonomic device constrains position as well as velocity, as for instance a $2:1$ gear pair does: we have both $2\theta_1 = \theta_2$ and $2\omega_1 = \omega_2$. A nonholonomic device constrains velocity but not position. For instance, a CVT may enforce $2\omega_1 = \omega_2$ when its transmission ratio $\alpha = 2$, but returning θ_1 to zero will not necessarily return θ_2 to zero, because α may have had other values in the interim.

ergonomics, increased productivity, and enhanced product quality.

A second application area of interest is image-guided surgery. One interesting technique in this field is the use of a robot to hold and position a tool guide. Once the robot has positioned the guide, a surgeon may introduce a tool through the guide and be confident that the tool is properly oriented. A cobotic tool guide holder may prove to be an even better platform owing to the cobot's passivity and intrinsically higher level of safety. Moreover, it is possible that virtual surfaces could be used instead of a physical tool guide. Recently, Emrich and Hodgson [5] have begun work on a novel cobot mechanism with the end goal of applying it to computer-assisted knee surgery.

A third application area may prove to be virtual prototyping, especially of large-scale systems such as automobile bodies. The intrinsic stability of cobotic virtual surfaces may prove to be an advantage when compared to conventional haptic devices. Work in this area has recently begun in our laboratory.

D. Open Questions and Future Work

There are a large number of questions relating to cobots, their control, and applications, which we hope will be investigated by our group and others. A few of these are the following.

Path Planning: Cobot path planning could be the creation of virtual surfaces rather than endpoint trajectories. How should such surfaces be created for a given task environment? Is this computationally easier than the general path planning problem?

Haptic Effects: In the discussion of the Unicycle cobot we pointed out that cobots, while ideally suited to smooth, hard virtual surfaces, are poorly suited to other haptic effects such as compliance, texture, and friction. Powered cobots, however, exhibit some of the properties of conventional haptic interfaces. What are the haptic capabilities of powered cobots?

Ergonomics: In "mutual labor" tasks, in which both significant operator forces and significant cobot forces act on a payload, how should the shape of the virtual surfaces be devised in order to minimize the stress on the human body, or perform the task most quickly, or with greatest dexterity?

CVT Design: While CVTs based on Rollerblade wheels have proven quite effective in prototype cobots, they can be quite bulky. Moreover, CVTs based on point-contact transmissions, including designs similar to those employed in cobots, are known to exhibit somewhat poor efficiencies in power-transmission applications [21], [22]. Of course, the primary role of CVTs used in cobots is constraint rather than power transmission, therefore, important topics of future research include the development of appropriate figures-of-merit as well as optimized designs.

Readers may also be interested in other questions related to CVT design [6] or cobot control [7].

ACKNOWLEDGMENT

REFERENCES

[1] N. H. Beachley and A. A. Frank, "Continuously variable transmissions: Theory and practice," Lawrence Livermore Lab., CA, OCLC: 06 690 884, 1979.

[2] W. Book, R. Charles, H. Davis, and M. Gomes, "The concept and implementation of a passive trajectory enhancing robot," *Proc. ASME Dyn. Sys. Cont. Div.*, vol. DSC-58, p. 633, 1996.

[3] J. E. Colgate and J. M. Brown, "Factors affecting the Z-width of a haptic display," in *Proc. IEEE 1994 Int. Conf. Robot. Automat.*, May 1994, pp. 3205–3210.

[4] Y. Delnondedieu and J. Troccaz, "PADyC: A passive arm with dynamic constraints: A prototype with two degrees of freedom," in *Proc. IEEE Conf. Med. Robotics Comp. Assisted Surgery*, 1995, pp. 173–180.

[5] R. Emrich and A. J. Hodgson, "A translational-to-rotational continuously variable transmission element for a parallel cobot," *Proc. ASME Dyn. Sys. Cont. Div.*, vol. DSC-69-2, pp. 1285–1292, 2000.

[6] R. B. Gillespie, C. A. Moore, M. A. Peshkin, and J. E. Colgate, "Kinematic creep in continuously variable transmissions: Traction drive mechanics for cobots," J. Mech. Syst. Design, submitted for publication.

[7] R. B. Gillespie, J. E. Colgate, and M. A. Peshkin, "A general framework for cobot control," *IEEE Trans. Robot. Automat.*, vol. 17, pp. 391–401, Aug. 2001.

[8] "Seventh annual symposium on haptic interfaces for virtual environment and teleoperator systems," Int. Mechan. Eng. Congress and Exposition, ASME, 1998.

[9] O. Haugwitz, "Variable speed drive transmissions of the frictional type," U.S. patent 2 727 396, 1955.

[10] R. Bajcsy, J. Canny, T. Fukuda, G. Giralt, R. Harrigan, K. Goldberg, and H. Moraff, (panel discussion), "The grand challenges for robotics and automation," in *Proc. IEEE 1996 Int. Conf. Robot. Automat.*, Minneapolis, MN, Apr. 1996.

[11] H. Kazerooni, "The human power amplifier technology at the University of California, Berkeley," *J. Robot. Automat. Syst.*, vol. 19, pp. 179–187, 1996.

[12] J. Kim, H. J. Yeom, and F. C. Park, "MOSTS: A mobile robot with a spherical continuously variable transmission," in *Proc. 1999 IEEE/RSJ Int. Conf. Intell. Robots Syst.*, vol. 3, 1999, pp. 1751–1756.

[13] C. A. Moore, "Continuously variable transmission for serial link cobot architectures," Master's thesis, Northwestern Univ., 1997.

[14] C. A. Moore, M. A. Peshkin, and J. E. Colgate, "Design of a 3R cobot using continuously variable transmissions," in *IEEE Int. Conf. Robot. Automat.*, 1999.

[15] T. E. Deeter, G. J. Koury, K. M. Rabideau, M. B. Leahy, Jr., and T. P. Turner, "The next generation munitions handler advanced technology demonstrator program," in *IEEE Intnl. Conf. Robot. Automat.*, 1997, pp. 341–345.

[16] "Proc. 1997 robotics industry forum," Robotics Institute of America, November 1997.

[17] L. B. Rosenberg, "Virtual fixtures: Perceptual tools for telerobotic manipulation," in *Proc. IEEE Virtual Reality Int. Symp. (VRAIS'93)*, 1993, pp. 76–82.

[18] M. A. Russo and A. Tadros, "Controlling dissipative magnetic particle brakes in force reflective devices," *Proc. ASME Dyn. Sys. Cont. Div.*, vol. DSC-42, pp. 63–70, 1992.

[19] C. Sayers, "Operator control of telerobotic systems for real world intervention," Ph.D. dissertation, The Univ. Pennsylvania, 1995.

[20] J. J. Soerdalen, Y. Nakamura, and W. J. Chung, "Design of a nonholonomic manipulator," in *Proc. IEEE Int. Conf. Robot. Automat.*, 1994.

[21] H. Tanaka, H. Machida, H. Hata, and M. Nakano, "Half-toroidal traction drive continuously variable power transmission for automobiles," *JSME Int. J.: Dyn., Contr., Robot., Design Manuf.*, ser. C, vol. 38, no. 4, pp. 772–777, 1995.

[22] H. Tanaka, M. Eguchi, H. Machida, and T. Imanishi, "Power transmission of a half-toroidal traction drive continuously variable transmission," *JSME Int. J.: Dyn., Contr., Robot., Design Manuf.*, ser. C, vol. 38, no. 4, pp. 778–782, 1995.

[23] J. E. Colgate, W. Wannasuphoprasit, and M. A. Peshkin, "Cobots: Robots for collaboration with human operators," *Proc. ASME Dyn. Sys. Cont. Div.*, vol. DSC-58, pp. 433–440, 1996.

[24] W. Wannasuphoprasit, P. Akella, M. A. Peshkin, and J. E. Colgate, "Cobots: A novel material handling technology," *ASME*, vol. 98-WA/MH-2, 1998.

Michael A. Peshkin (S'86–M'86) received the Ph.D. degree in physics from Carnegie-Mellon University, Pittsburgh, PA, in 1987.

He is currently an Associate Professor in the Department of Mechanical Engineering at Northwestern University, Evanston, IL. With colleague J. E. Colgate, he is an inventor of cobots and a founder of Cobotics, Inc. He is also a founder of Z-KAT, Inc., in the image-guided surgery field. He holds patents on cobots, image-guided surgery, and electromagnetic sensors. Among current projects, he is working with the Robotics Industries Association, creating a national safety standard for intelligent assist devices.

Dr. Peshkin has served as Associate Editor of IEEE TRANSACTIONS ON ROBOTICS AND AUTOMATION and was for several years the Conference Publications Editor of IEEE Control Systems Society (ACC and CDC conferences).

J. Edward Colgate (M'88) received the Ph.D. degree in mechanical engineering from the Massachusetts Institute of Technology, Cambridge, in 1988.

He subsequently joined Northwestern University, Evanston, IL, where he is currently an Associate Professor with the Department of Mechanical Engineering. His principal research interests are cobots—collaborative robots—and haptic interface. In addition to his academic pursuits, he is a founder of Cobotics, Inc., a leading developer of human interface technologies for the industrial marketplace.

Dr. Colgate has served as an Associate Editor for the IEEE TRANSACTIONS ON ROBOTICS AND AUTOMATION. He has served as U.S. Editor of *Robotics and Computer Integrated Manufacturing* and as an Associate Editor of the *Journal of Dynamic Systems, Measurement and Control*.

Witaya Wannasuphoprasit was born in Bangkok, Thailand, in 1967. He received the Bachelor degree from King Mongkut's Institute of Technology, Ladkrabang, Bangkok, Thailand, in 1990 and the M.S. and Ph.D. degrees from Northwestern University, Evanston, IL, in 1993 and 1999, respectively, all in mechanical engineering.

From 1999 to 2000, he was a Postdoctoral Fellow with t Northwestern University conducting research on cobots and "Intelligent Assist Devices." Currently, he is a Lecturer with the Mechanical Engineering Department, Chulalongkorn University, Bangkok. His fields of research include cobots, haptic interfaces, and the interaction of humans with intelligent systems.

Dr. Wannasuphoprasit received the Best Paper Award from the IEEE International Conference on Robotics and Automation in 1996 and the Best Paper Award from the ASME International Mechanical Engineering Congress and Exposition (MHED Division) in 1998. He is a coeditor of the *Journal of the Thai Robotics Association*.

Carl A. Moore received the B.S. degree in mechanical engineering from Howard University, Washington, DC, and the M.S. and Ph.D. degrees from Northwestern University, Evanston, IL.

As a graduate student in the Laboratory for Intelligent Mechanical Systems, he studied the mechanical characteristics of a continuously variable transmission used in revolute jointed cobots. He recently designed and built the first arm-like cobot. His research interests include the design and control of intelligent assist devices for use in manufacturing, industrial design, and surgical robotics. He is currently an Assistant Professor with the Department of Mechanical Engineering, Florida State University, Tallahassee.

R. Brent Gillespie (M'96) received the B.S. degree in mechanical engineering from the University of California at Davis in 1986, the Master's degree in music (piano performance) from the San Francisco Conservatory of Music in 1989, and the Masters and Ph.D. degrees in mechanical engineering in 1992 and 1996, respectively, from Stanford University, Stanford, CA.

Prior to beginning his graduate studies, he spent four years with Hewlett Packard, San Jose, CA. From 1996 to1999, he held an NSF-sponsored Postdoctoral Fellowship with Northwestern University, Evanston, IL. Since September 1999, he began his present position as an Assistant Professor of mechanical engineering with the University of Michigan, Ann Arbor. His research interests include haptic interface and cobots.

Dr. Gillespie has received a National Science Foundation CAREER Award.

Prasad Akella (S'87–M'90) received the B.S. degree from the Indian Institute of Technology, the M.B.A. degree (with highest distinction) from the Michigan Business School, and the M.S. and Ph.D. degrees from Stanford University, Stanford, CA.

He is a Principal Product Manager at Commerce One (C1). He is responsible for product and product strategy for C1's electronic marketplace-based design and supply chain tools. He was a Staff Engineer in General Motors' Robotics Department and led the Intelligent Assist Device (IAD) Project since inception in 1995. Prior to GM, he was a NSF-STA Fellow at MITI's Mechanical Engineering Laboratory in Japan.

Dr. Akella was awarded GM's highest technical award—the "Boss" Kettering Award—for developing the IAD technology. He has also won the ASME Material Handling Engineering Division's Best Conference Paper Award and the Anton Philips Best Student Paper Award of the IEEE Robotics and Automation Society. He was an Edward Meakin Fellow at Stanford and was awarded the HAL Silver Medal by the Indian Institute of Technology. He serves on the editorial board of the *Robotics and Computer Integrated Manufacturing Journal* and on CommerceNet's Evolving Supply Chain Advisory Panel. He was the founding Vice-Chair of the IAD ANSI Safety Standards Committee.